Iron-Substituted Lithium Titanium Spinels: Structural and Electrochemical Characterization

P. Reale,*,† S. Panero,† F. Ronci,‡ V. Rossi Albertini,‡ and B. Scrosati†

Dipartimento di Chimica, Università degli Studi di Roma "La Sapienza", P.le A.Moro 5, 00185 Roma, Italy, and Istituto di Struttura della Materia - CNR, via del Fosso del Cavaliere 100, 00133 Roma, Italy

Received March 6, 2003. Revised Manuscript Received June 18, 2003

Iron-substituted lithium titanium spinels with stoichiometry $Li_{4/3-y/3}Fe_yTi_{5/3-2y/3}O_4$, were synthesized by a sol gel process. The attention was focused on two compositions, namely $Li_{1.3}Fe_{0.1}Ti_{1.6}O_4$ and $Li_{1.25}Fe_{0.25}Ti_{1.5}O_4$. The first spinel crystallizes in the typical $Fd\bar{3}m$ space group while the second adopts the $P4_332$ symmetry. The two spinels were tested as electrodes in lithium cells. It was observed that these electrodes are capable of inserting up to 1.4−1.6 lithium ion equivalents per formula unit and to cycle reversibly 160−180mAh/g at C/5 in the 2.9−0.2 V potential range. The electrochemical responses are quite different from that of pure $Li_{4/3}Ti_{5/3}O_4$, since the lithium insertion (deinsertion) processes evolve through several one-phase and two-phase steps, clearly involving the reduction (oxidation) of both titanium (IV) and iron (III) which occupy different framework positions. The electrochemical discharge mechanism of the two spinel electrodes was investigated by combining electrochemical tests with in situ diffraction measurements carried out using high-energy synchrotron radiation.

Introduction

Lithium titanium spinels are very appealing electrode materials for lithium ion batteries. Considerable attention has been devoted to the $Li[Li_{1/3}Ti_{5/3}]O_4$ compound with the investigation of its electrochemical behavior in cells, using either liquid[1−5] or polymer electrolytes.[6−7] As extensively reported,[3,9−11] the main feature of this compound is the unique insertion−deinsertion mechanism that involves a two-phase process between two compounds having the same symmetry. The lattice parameter variation associated with this process is confined to less than 0.1%, to the point that $Li[Li_{1/3}Ti_{5/3}]O_4$ has been classified as a "zero-strain" intercalation compound.[2]

Following this trend, there have been a few reported investigations dealing with substituted spinel with the general stoichiometry $Li_{4/3-y/3}M_yTi_{5/3-2y/3}O_4$ and aiming to clarify the effect of the partial substitution of lithium and titanium with a trivalent transition metal ion (e.g., Fe^{3+}, Ni^{3+}, and Cr^{3+}) on the crystal structure[12] and on the electrochemical performances.[13−15] Of particular interest are the substitutions with iron, i.e., an abundant, nontoxic electroactive element, that confers to the spinel singular electrochemical properties.[13] Accordingly, $Li_{4/3-y/3}M_yTi_{5/3-2y/3}O_4$ has been synthesized by a solid-state route in two different cubic space groups: (i) the ideal spinel $Fd\bar{3}m$ for $0 < y < 0.15$ and $0.7 < y < 1.9$; and (ii) a less symmetrical cubic cell $P4_332$ for $0.15 < y < 0.7$ and $1.9 < y < 2.5$, isotypic to $Li_{0.5}Fe_{2.5}O_4$.[12] However, only a few stoichiometries have been tested in lithium batteries[13] and, to our knowledge, none of the $P4_332$ symmetry.

In this paper we report the results of a study carried out by electrochemical and structural investigations on iron-substituted lithium titanium spinels having the $Li_{4/3-y/3}M_yTi_{5/3-2y/3}O_4$ general formula. We have considered two different stoichiometries, namely $Li_{1.3}Fe_{0.1}Ti_{1.6}O_4$ ($Fd\bar{3}m$) and $Li_{1.25}Fe_{0.25}Ti_{1.5}O_4$ ($P4_332$), both prepared by a sol gel synthetic route.

* Corresponding author. E-mail: priscilla.reale@uniroma1.it.
† Università degli Studi di Roma "La Sapienza".
‡ Istituto di Struttura della Materia - CNR.

(1) Colbow, K. M.; Dahn, J. R.; Haering, R. R. *J. Power Sources* **1989**, *26*, 397−402.
(2) Ohzuku, T.; Ueda, A.; Yamamoto, N. *J. Electrochem. Soc.* **1995**, *142* (5), 1431−1435.
(3) Sharner, S.; Weppner, W.; Schmid-Beurmann, P. *J. Electrochem. Soc.* **1999**, *146* (3), 857−861.
(4) Bach, S.; Pereira-Ramos, J. P.; Baffier, N. *J. Power Sources* **1999**, *81−82*, 273−276.
(5) Pyun, S. I.; Kim, S. W.; Shin, H. C. *J. Power Sources* **1999**, *81−82*, 248−254.
(6) Peramunage, D.; Abraham, K. M. *J. Electrochem. Soc.* **1998**, *145* (8), 2615−2622.
(7) Zaghib, K.; Simoneau, M.; Armand, M.; Gauthier, M. *J. Power Sources* **1999**, *81−82*, 300−305.
(8) Robertson, A. D.; Trevino, L.; Tukamoto., H.; Irvine, J. T. S. *J. Power Sources* **1999**, *81−82*, 352−357.
(9) Panero, S.; Reale, P.; Ronci, F.; Scrosati, B.; Perfetti, P.; Rossi Albertini, V. *Phys. Chem. Chem. Phys.* **2001**, *3*, 845−847.
(10) Rossi Albertini, V.; Perfetti, P.; Ronci, F.; Reale, P.; Scrosati, B. *Appl. Phys. Lett.* **2001**, *79* (1), 27−29.
(11) Ronci, F.; Reale, P.; Scrosati, B.; Panero, S.; Rossi Albertini, V.; Perfetti, P.; di Michiel, M.; Merino, J. M. *J. Phys. Chem. B* **2002**, *106*, 3082−3086.
(12) Sharner, S.; Weppner, W.; Schmid-Beurmann, P. *J. Solid State Chem.* **1997**, *134*, 170−181.
(13) Robertson, R. D.; Tukamoto, H.; Irvine, J. T. S. *J. Electrochem. Soc.* **1999**, *146* (11), 3958−3962.
(14) Arillo, M. A.; Lopez, M. L.; Perez-Cappe, E.; Pico, C.; Veiga, M. L. *Solid State Ionics* **1998**, *107*, 307−312.
(15) Ohzuku, T.; Tatsumi, K.; Matoba, N.; Sawai, K. *J Electrochem. Soc.* **2000**, *147* (10), 3592−3597.

10.1021/cm034122c CCC: $25.00
Published on Web 08/05/2003

Experimental Section

Lithium iron titanium spinels were synthesized by sol−gel technique carried out by mixing in ethanol a stoichiometric amount of titanium isopropoxide $Ti(OCH(CH_3)_2)_4$ (Aldrich 97%), lithium acetate $CH_3COOLi·H_2O$ (Aldrich 98%), and $Fe(NO_3)_3·9H_2O$. A sort of polymerization occurs with the formation of a reddish gel. This gel was preliminarily dried at mild temperatures and then the product was annealed at 800° for 16 h in oxygen atmosphere. The so-obtained powders were analyzed by X-ray powder diffraction (Rigaku Miniflex using Cu Kα radiation).

The electrodic membranes were prepared by blending the spinel active material with PVdF 6020 (Solef Solvay) as the binder and with Super P as the electronic conductor, in an 83:12:5 weight ratio. The three components were carefully dispersed in *N*-methyl-2-pyrrolidinone (NMP) and the mixture was spread on a copper foil with the so-called "doctor blade" technique. After solvent evaporation, electrode disks were cut and dried at 120 °C under vacuum. The test cells were assembled using high-purity lithium foil as the counter and the reference electrode and a 1 M $LiClO_4$ solution in EC/DEC (1:1) as the electrolyte. The electrochemical characterization consisted of potentiodynamic (PCGA) and galvanostatic (GC) cyclations carried out in the 0.2−2.9 V vs Li^+/Li voltage range using a VMP (Biologic SA) and a Maccor systems, respectively.

In situ XRD measurements were performed at the ID15B beam line of the European Synchrotron Radiation Facility using an experimental setup described elsewhere.[10,11] The cell is almost totally transparent to the high-energy (∼88 keV) monochromatic primary X-ray beam,[10] this being an additional and unique practical advantage of the technique. Furthermore, the use of a read-out image plate detector (model MAR 345) guarantees a fast collection of the Debye−Sharrer rings and, consequently, a dense time sampling of the evolution of the structure upon the progress of the electrochemical process. The images of the Debye−Sharrer rings were then converted into the corresponding diffraction patterns by radial integration. The experimental method consisted of collecting in situ a sequence of diffractograms produced by the evolving lattice structure of the active material during the first three galvanostatic cycles of the test cell. The cycles were controlled by an AMEL 545 galvanostat using a constant current equivalent to a C/5 rate in the 2.9−1.2 V range for the first cycle and 2.9−0.2 V range for the following two cycles. The computer-controlled acquisition system allowed the collection of a single pattern every 125 s (40 s for the actual acquisition and 85 s for data downloading). In this way a high sampling rate was assured, in turn allowing an almost constant composition during the acquisition of a single pattern. In fact, in the course of 125 s the x variation in the $Li_{4/3-y/3+x}M_yTi_{5/3-2y/3}O_4$ electrode was less than 0.007.

Two sets of diffraction data were obtained, one for $Li_{1.3}Fe_{0.1}Ti_{1.6}O_4$ and the other for $Li_{1.25}Fe_{0.25}Ti_{1.5}O_4$. The patterns were analyzed with the aid of a Rietveld software made in-house.

Results and Discussion

Two compounds with different iron contents have been synthesized: $Li_{1.3}Fe_{0.1}Ti_{1.6}O_4$ and $Li_{1.25}Fe_{0.25}Ti_{1.5}O_4$. Figure 1 shows the X-ray diffraction patterns of the two compounds. Because iron and titanium have very close X-ray scattering factors, it is not possible by Rietveld refinement of the XRD patterns to distinguish the positions of the two ions; then, the refinement was carried out assuming that Ti(IV) has the tendency to occupy octahedral sites, as also proposed by Sharner et al.[12] In the $P4_332$ network of the $Li_{1.25}Fe_{0.25}Ti_{1.5}O_4$ the 4b positions were attributed to lithium[12] and the location of Li and Fe in the remaining sites was refined. The distribution proposed in their paper is the one that gives the best fit. Of course neutron scattering would allow a much better refinement of the structure and we are planning to carry out this experiment soon.

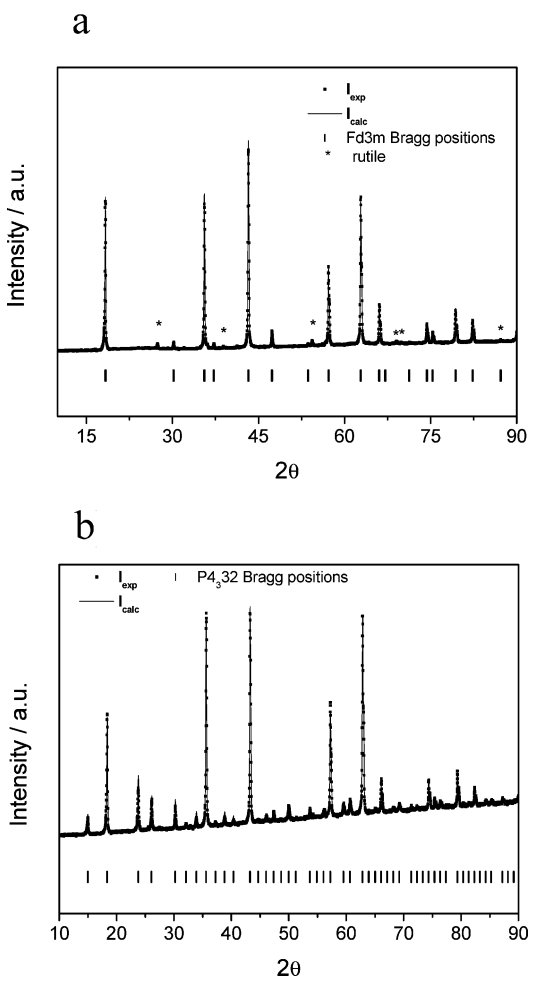

Figure 1. X-ray powder diffraction of the as-synthesized $Li_{1.3}Fe_{0.1}Ti_{1.6}O_4$ (a) and $Li_{1.25}Fe_{0.25}Ti_{1.5}O_4$ (b). Calculated patterns are reported together with the experimental curves. Rutile content below 2%.

The structures of the two compounds are different. Similarly to $Li_{4/3}Ti_{5/3}O_4$, $Li_{1.3}Fe_{0.1}Ti_{1.6}O_4$ crystallizes in the $Fd\bar{3}m$ space group, with a comparable lattice parameter, $a = 8.3607(1)$Å. The analysis shows a small inverse character for $Li_{1.3}Fe_{0.1}Ti_{1.6}O_4$, as most of the iron occupies tetrahedral 8a positions, leading to a stoichiometry that can be written as $(Li_{0.91}Fe_{0.09})_{(8a)}[Li_{0.39}Fe_{0.01}Ti_{1.6}]_{(16d)}O_{4(32e)}$. The small amount of rutile TiO_2 detected in the $Li_{1.3}Fe_{0.1}Ti_{1.6}O_4$ XRD pattern has been considered negligible. On the contrary, $Li_{1.25}Fe_{0.25}Ti_{1.5}O_4$ results isotypic to $Li_{0.5}Fe_{2.5}O_4$ and thus, it can be indexed in the $P4_332$ cubic space group with a lattice parameter $a = 8.3592(1)$Å. The formula can be written as $Li_{0.5(4b)}(Li_{0.75}Fe_{0.25})_{(8c)}\ Ti_{1.5(12d)}O_{4(8c,\ 24e)}$.

Figure 2 shows models of the two structures. Both have a cubic close-packed oxygen array with nearly identical unit cell ($Z = 8$) and lattice parameter. In the $Fd\bar{3}m$ space group the edge sharing octahedral positions can be either randomly occupied by different cations

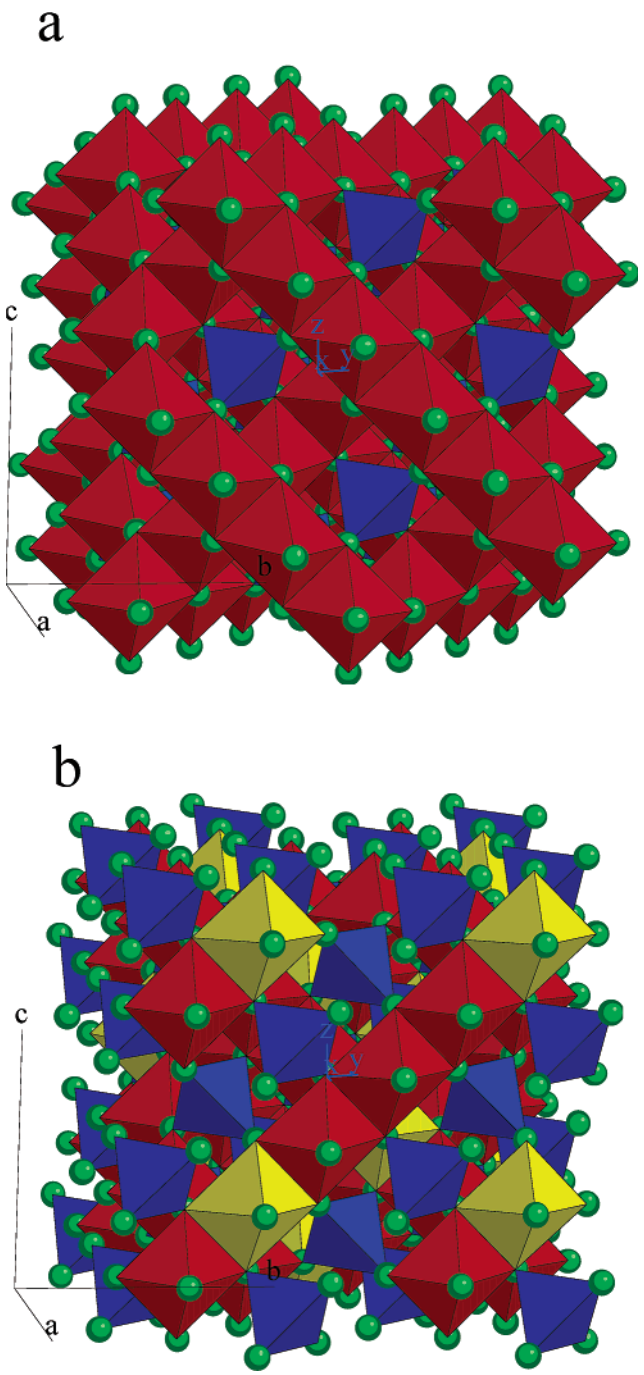

Figure 2. Models of the structures of $Li_{1.3}Fe_{0.1}Ti_{1.6}O_4$ (a) and $Li_{1.25}Fe_{0.25}Ti_{1.5}O_4$ (b). In the $Fd\bar{3}m$ structure (a) blue tetrahedra represent the 8a position and the 16d octahedra are in red; in the $P4_332$ structure (b) the 8c tetrahedra are blue, the 4b lithium octahedra are yellow, and 12d titanium octahedra are red.

(16d colored in red in Figure 2) or totally empty (16c). Conversely, the $P4_332$ space group is characterized by a lower symmetry since edge sharing octahedral positions can be distinguished in the 12d and 4b sites or, alternatively, in the 12d and 4a sites. The 12d and 4a sites are empty in $Li_{1.25}Fe_{0.25}Ti_{1.5}O_4$, while the 12d (red octahedra) and the 4b (yellow octahedra) sites are occupied by titanium and lithium, respectively. In both phases, $^1/_8$ of the tetrahedral positions are randomly occupied by lithium and iron; these positions are the 8a sites in the $Fd\bar{3}m$ and the 8c sites in the $P4_332$ (see

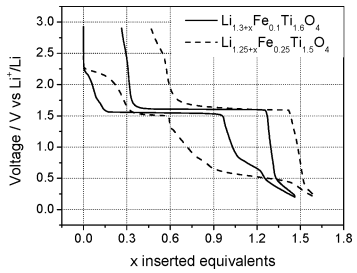

Figure 3. Voltage profiles obtained by potentiodynamic cycling with galvanostatic acceleration of $Li_{1.3}Fe_{0.1}Ti_{1.6}O_4$ and $Li_{1.25}Fe_{0.25}Ti_{1.5}O_4$ electrodes. Voltage range: 2.9−0.2 V vs Li^+/Li. ΔE = 10 mV, i_l = C/20. Counter and reference electrode: lithium metal. Electrolyte: $LiClO_4$ 1 M in EC/DEC (1:1).

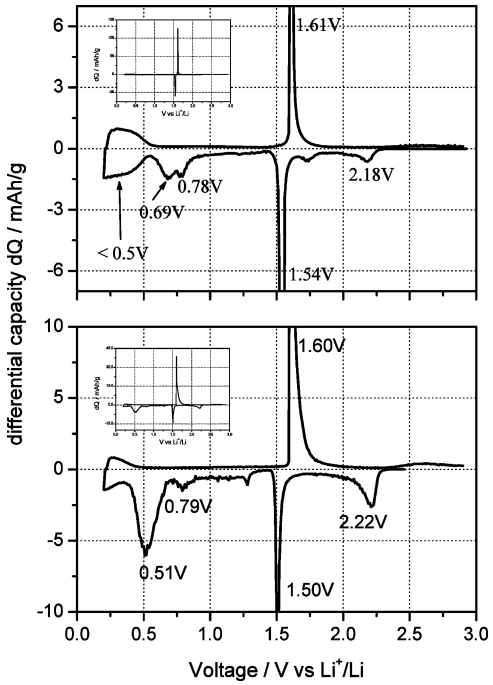

Figure 4. Differential capacity plot derived from Figure 3.

blue tetrahedra in Figure 2). Such sites share faces with the empty octahedral sites, so it is presumable that, as in $Li_{4/3}Ti_{5/3}O_4$, the Li^+ insertion is accompanied by migration of ions from the pristine tetrahedral to the empty octahedral positions.

Actually, electrochemical tests support the hypothesis of a two-phase lithium insertion−deinsertion process, as typically observed in the case of $Li_{4/3}Ti_{5/3}O_4$, even if in a more complex fashion. In fact, the discharge and recharge processes occur through a complex sequence of steps. As shown by the voltage and differential capacity profiles reported in Figures 3 and 4 respectively, the first discharge of both the compounds can be described by the following step sequence: (a) a first process around 2.2 V vs Li^+/Li not totally reversible; (b) a plateau (corresponding to a peak in the differential capacity plot, see Figure 4) at 1.5 V vs Li^+/Li; (c) a process around 0.78−0.79 V vs Li^+/Li present only in the first one or two cycles; (d) a second plateau at low voltages (~0.69 V for $Li_{1.3}Fe_{0.1}Ti_{1.6}O_4$ and 0.51 V vs Li^+/Li for $Li_{1.25}Fe_{0.25}Ti_{1.5}O_4$); and (e) a process near the cutoff voltage.

Process (a) is possibly related to Fe^{3+}/Fe^{2+} reduction. In fact, it does not occur in $Li_{4/3}Ti_{5/3}O_4$[1−7] and its

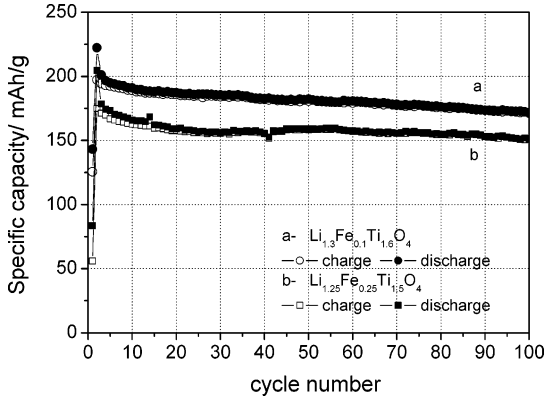

Figure 5. Galvanostatic cycling at C/5 of $Li_{1.3}Fe_{0.1}Ti_{1.6}O_4$ and $Li_{1.25}Fe_{0.25}Ti_{1.5}O_4$ electrodes. Voltage range: 2.9−0.2 V. Counter electrode: lithium metal. Electrolyte: $LiClO_4$ 1 M in EC/DEC (1:1).

amplitude is proportional to the iron content. The plateau (b) is attributed to Ti^{4+}/Ti^{3+} reduction. However, although this plateau is wide in the case of $Li_{1.3}Fe_{0.1}$-$Ti_{1.6}O_4$, it has a comparatively smaller extension for $Li_{1.25}Fe_{0.25}Ti_{1.5}O_4$. On the other hand, for the latter it is the next following region around 1 V, where the voltage shows a slight continuous decrease, which becomes important. This behavior can be accounted for by considering that ions migrate from the tetrahedral 8c sites to the octahedral 12d sites, which can host only 1.5 atoms per formula unit. Therefore, if one equivalent of cations comes from the 8c positions, only 0.5 extra lithium ions can be inserted during the step. The other 0.5 equiv can be subsequently inserted in the 4a octahedral positions through a process that is topotactic and does not involve further rearrangements.

Process (c) is probably promoted by the Super P[17] added in the electrode film (see Experimental Section). Process (d), while typical of substituted spinels,[13] slightly differs for the two compounds examined here, depending on the symmetry and the iron content. It is possible that the redox couple involved in this process is Fe^{2+}/Fe^0, as its intensity is related to the iron substitution. Finally, process (e) is similar to that usually observed in the not-substituted $Li_{4/3}Ti_{5/3}O_4$ spinel.[16,17]

The reproducibility and the efficiency of the whole lithium insertion−deinsertion process can be evaluated through the galvanostatic cyclation reported in Figure 5. At C/5 the capacity delivered is remarkably high and stable upon long cycling: at the 100th cycle the discharged capacity of $Li_{1.3}Fe_{0.1}Ti_{1.6}O_4$ is still around 170 mAh/g while that for $Li_{1.25}Fe_{0.25}Ti_{1.5}O_4$ is around 150 mAh/g. It may be assumed that the lower performance of the $Li_{1.25}Fe_{0.25}Ti_{1.5}O_4$ electrode is not due to the small differences in the symmetry, but rather to the higher iron content, to which a poor reversible electroactivity may be associated.

To further investigate the structural changes upon lithium insertion, we have carried out an in situ diffraction experiment performed at the ID15B beam

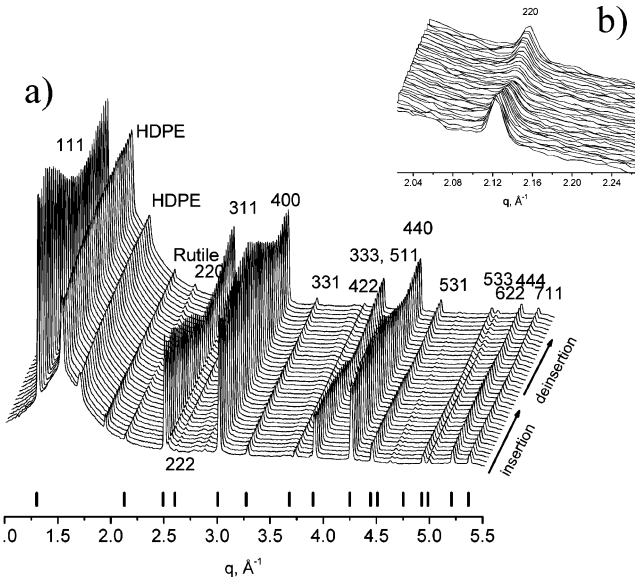

Figure 6. X-ray pattern diffraction sequence collected during a galvanostatic cycle of a $Li_{1.3}Fe_{0.1}Ti_{1.6}O_4$ electrode. Rate: C/5. Voltage range: 2.9−0.2 V. Counter electrode: lithium metal. Electrolyte: 1 M $LiClO_4$ in EC/DEC (1:1). Figure 6b evidences detail of the 220 Bragg peak.

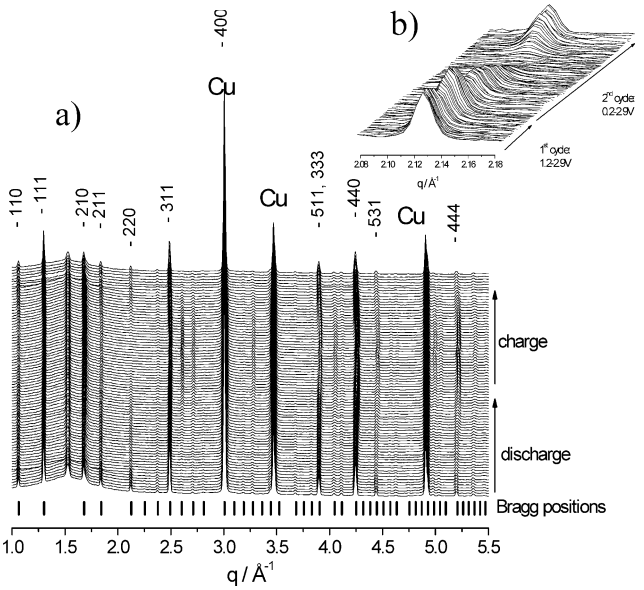

Figure 7. X-ray pattern diffraction sequence collected during a galvanostatic cycle of a $Li_{1.25}Fe_{0.25}Ti_{1.5}O_4$ electrode. Rate: C/5. Voltage range: 2.9−0.2 V. Counter electrode: lithium metal. Electrolyte: 1 M $LiClO_4$ in EC/DEC (1:1). Figure 7b evidences detail of the evolution of the 220 Bragg peak.

line of the European Synchrotron Radiation Facility. Both spinels were tested to detect the lattice changes as a function of the Li insertion level; to achieve this goal, the first discharge was limited to 1.2 V to focus the attention on the two-phase process, but in the following two cycles discharge was extended to 0.2 V.

Figures 6 and 7 show the sequence of the collected spectra. No meaningful changes in the diffraction pattern are observed even at high insertion levels. The main effects are: (i) periodic and concerted variation in the peak intensities, following the changes in population of the crystallographic sites, and (ii) minor variations in the peaks' positions (Figures 6a and 7a). The intensity variations show the reversible disappearance

(16) Reale, P. Ph.D. Thesis, Università degli Studi di Roma "La Sapienza", Rome, 2002.
(17) Robertson, A. D.; Trevino, L.; Tukamoto, H.;Irvine, J. S. *J. Power Sources* **1999**, *81−82*, 352.

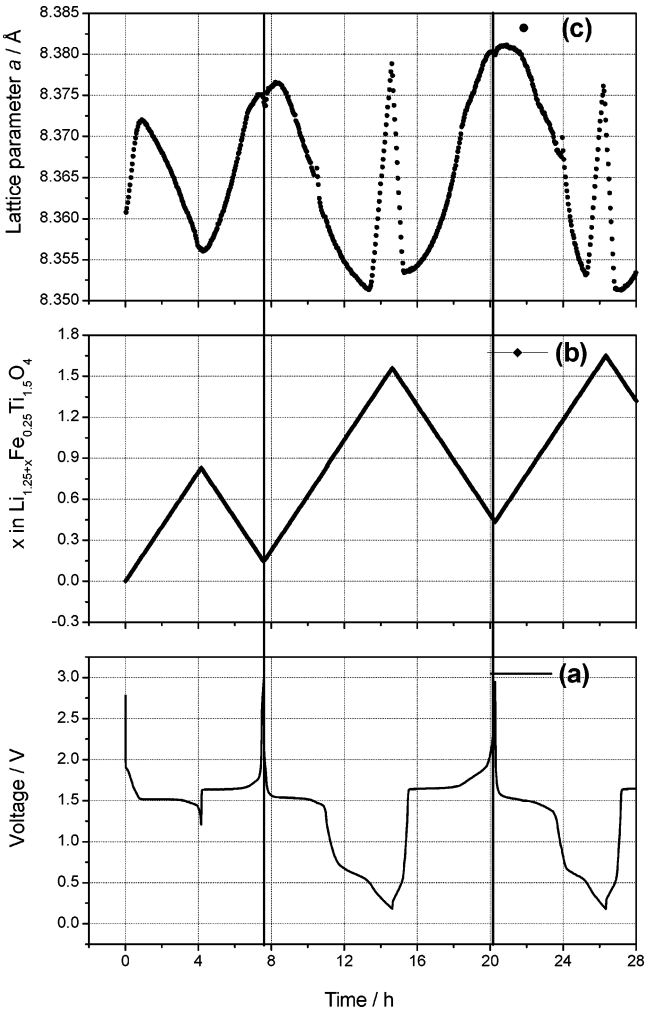

Figure 8. Lattice parameter evolution (c) of $Li_{1.3}Fe_{0.1}Ti_{1.6}O_4$ during three galvanostatic cycles as a function of voltage (a) and of the lithium insertion level (b).

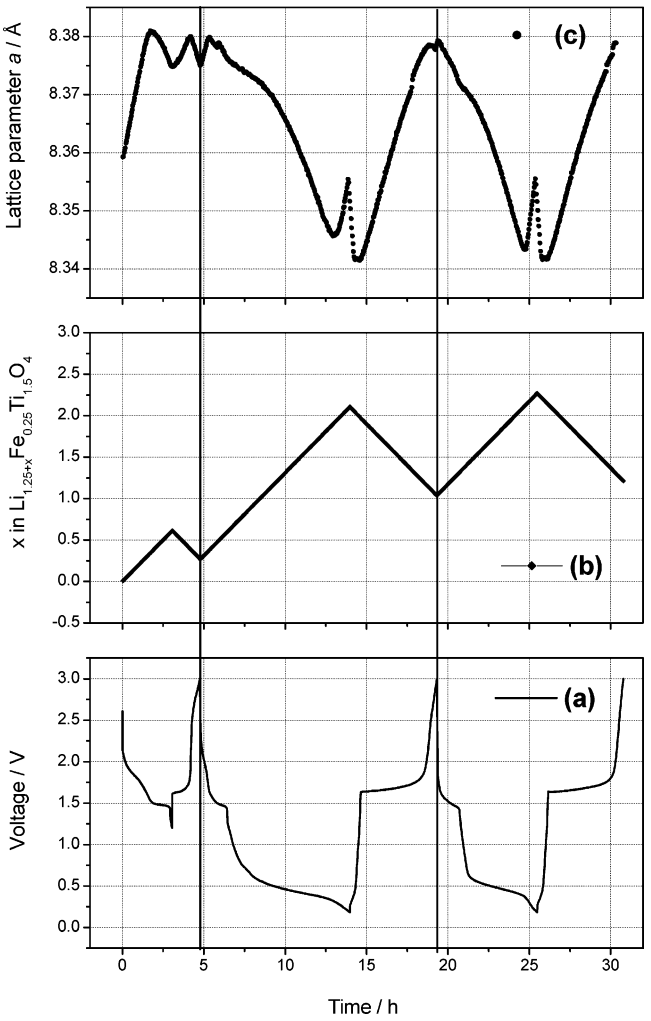

Figure 9. Lattice parameter evolution (c) of $Li_{1.25}Fe_{0.25}Ti_{1.5}O_4$ during three galvanostatic cycles as a function of voltage (a) and of the lithium insertion level (b).

upon voltage excursion of the 220 Bragg peak (Figures 6b and 7b); considering that this peak is related to atoms in tetrahedral positions,[18] the results confirm that at the beginning of the insertion process the iron ions move in coherence with the lithium ions.

The two compounds retain their original symmetry for the entire dicharge−charge cycles, allowing a straightforward processing of the spectra for obtaining the trends of the lattice parameter of $Li_{1.3+x}Fe_{0.1}Ti_{1.6}O_4$ and of $Li_{1.25+x}Fe_{0.25}Ti_{1.5}O_4$ as a function of the voltage and the insertion level. Figures 8 and 9 show these trends and confirm the complex mechanism through which the Li insertion process takes place. At high voltage, this Li insertion process is accompanied by events similar to those observed for $Li_{4/3}Ti_{5/3}O_4$,[9−11] namely: (i) expansion of the pristine lattice due to an initial solubility of lithium, followed by (ii) a linear contraction of the *a* parameter due to the rearrangement of the cations for the formation of the lithium-rich phase. Then, for both compounds, the average $\bar{a}$ lattice parameter is $\bar{a} = (1 - x) \cdot a_1 + x \cdot a_2$. Bearing in mind the electrochemical behavior and the reversible disappearance of the 220 peak, in analogy to $Li_{4/3}Ti_{5/3}O_4$[9−11] we propose the following reaction sequence to account for the high voltage (>1.2 V) processes:

$$[Li_{0.91}Fe_{0.09}]_{(8a)}[Li_{0.39}Fe_{0.01}Ti_{1.6}]_{(16d)}O_{4(32e)} + \delta Li^+ + \delta e^- \leftrightarrow Li_{\delta(16c)}[Li_{0.91}Fe_{0.09}]_{(8a)}[Li_{0.39}Fe_{0.01}Ti_{1.6}]_{(16d)}O_{4(32e)} \quad (1a)$$

$$Li_{\delta(16c)}[Li_{0.91}Fe_{0.09}]_{(8a)}[Li_{0.39}Fe_{0.01}Ti_{1.6}]_{(16d)}O_{4(32e)} + (1\text{-}\delta)Li^+ + (1\text{-}\delta)e^- \leftrightarrow [Li_{1.91}Fe_{0.09}]_{(16c)}[Li_{0.39}Fe_{0.01}Ti_{1.6}]_{(16d)}O_{4(32e)} \quad (2a)$$

$$Li_{0.5(4b)}[Li_{0.75}Fe_{0.25}]_{(8c)}\ Ti_{1.5(12d)}O_{4(8c,\ 24e)} + \delta Li^+ + \delta e^- \leftrightarrow Li_{\delta(12d)}Li_{0.5(4b)}[Li_{0.75}Fe_{0.25}]_{(8c)}\ Ti_{1.5(12d)}O_{4(8c,\ 24e)} \quad (1b)$$

$$Li_{\delta(12d)}Li_{0.5(4b)}[Li_{0.75}Fe_{0.25}]_{(8c)}\ Ti_{1.5(12d)}O_{4(8c,\ 24e)} + (0.5\text{-}\delta)Li^+ + (0.5\text{-}\delta)e^- \leftrightarrow Li_{0.5(4b)}[Li_{1.25}Fe_{0.25}]_{(12d)}\ Ti_{1.5(12d)}O_{4(8c,\ 24e)} \quad (2b)$$

Reactions indexed with "a" are related to $Li_{1.3}Fe_{0.1}Ti_{1.6}O_4$, and those indexed with "b" are related to $Li_{1.25}Fe_{0.25}Ti_{1.5}O_4$. Unlike the case of the simple $Li_{4/3}Ti_{5/3}O_4$, processes (1a) and (1b), which are associated with event-(i), are almost irreversible since the expansion that

(18) Tarascon, J. M.; McKinnon, W. R.; Coowar, F.; Bowmer, T. N.; Amatucci, G.; Guyomard, D. *J. Electrochem. Soc.* **1994**, *142*, 1421.

occurs during insertion is not re-adsorbed during the following deinsertion process.

Event (ii) is represented by equations (2a) and (2b). Process (2b) is followed by the topotactic insertion which corresponds to the Li occupation of octahedral 4a sites. In this step, the *a* lattice parameter continues to decrease (Figure 9c). This can be described by the following equation:

$$Li_{0.5(4b)}[Li_{1.25}Fe_{0.25}]_{(8c)}\ Ti_{1.5(12d)}O_{4(8c,\ 24e)} + 0.5Li^{+} + 0.5e^{-} \leftrightarrow Li_{0.5(4a)}Li_{0.5(4b)}[Li_{1.25}Fe_{0.25}]_{(12d)}\ Ti_{1.5(12d)}O_{4(8c,\ 24e)} \quad (2.1b)$$

After the insertion of 1 equiv of lithium ions, all octahedral positions in the spinels are occupied. Further insertion is possible only at low voltages (0.7−0.5 V), to which a deeper contraction of the lattice is associated. As already hypothesized, here the reduction may involve Fe^{2+}/Fe^{0}. The deep insertion process is very complex and the X-ray diffraction analysis alone is not sufficient to fully clarify it; indeed, if nanosized, iron cannot be detected by X-ray. It is only possible to conclude that there is no evidence of formation of a new crystalline phase, nor of any important distortion of the pristine lattice. We believe that iron is extruded from the structure and substituted by the inserted lithium ions, according to

$$Li_{2.3}Fe_{0.1}Ti_{1.6}O_4 + qLi^{+} + qe^{-} \leftrightarrow Li_{2.3+q}Fe_{0.1-p}Ti_{1.6}O_4 + pFe^{0} \quad (3a)$$

$$Li_{2.25}Fe_{0.25}Ti_{1.5}O_4 + qLi^{+} + qe^{-} \leftrightarrow Li_{2.25+q}Fe_{0.25-p}Ti_{1.5}O_4 + pFe^{0} \quad (3b)$$

At the and of the discharge there is a reversible expansion, a phenomenon also observed for $Li_{4/3}Ti_{5/3}O_4$.[16,17] Again, XRD is not conclusive because no meaningful changes in the diffraction pattern are noticed. We may propose that insertion of some lithium ions could occur through either a topotactic process toward interstitial tetrahedral sites or a phase separation leading to a rock-salt anion deficient species.

It must be stressed that all the structural changes above-discussed imply an overall variation of the *a* parameter confined within 0.4%, a value higher than that observed in $Li_{4/3}Ti_{5/3}O_4$,[9−11] but still very low compared to the majority of the Li insertion electrodes.[19]

Conclusions

Two iron-substituted lithium titanium spinels, crystallizing in the $Fd\bar{3}m$ and the $P4_332$ space groups, have been synthesized through a sol−gel technique. The electrochemical response shown by the two spinels is complex, as the Li insertion and deinsertion process appears to evolve through several one-phase and two-phase reactions, involving the reduction/oxidation of both the titanium and the iron which occupy different framework positions. Even if a partial irreversibility related to the redox activity of iron has been observed, the electrochemical performance of both the compounds is quite interesting, considering capacity values as high as 150−170 mAh/g can be reversibly obtained over a hundred cycles. Such a long cycle life is obviously a consequence of the structural stability of the spinels that undergo very little strain during the repeated insertion−deinsertion cycles. Indeed, by in situ high-energy X-ray diffraction analysis carried out in ESRF, the minimal lattice deformation (below 0.4%) occurring upon cycling could be detected.

Acknowledgment. This work has been carried out with the financial support of the Italian Ministry of University and Research, MIUR, COFIN 2002. We also thank ESRF for financial support for the X-ray diffraction measurements and Dr. Marco di Michiel for the technical help provided.

CM034122C

(19) Rossi Albertini, V.; Perfetti, P.; Ronci, F.; Scrosati, B. *Chem. Mater.* **2001**, *13*, 450.